



RESEARCH ARTICLE

WILEY

Bond behaviour of rebar in concrete at elevated temperatures: A soft computing approach

Rwayda Kh. S. Al Hamd¹  | Saif Alzabeebee²  | Lee S. Cunningham³  | John Gales⁴ 

¹Abertay University School of Applied Sciences Dundee, Dundee, UK

²Department of Roads and Transport Engineering, College of Engineering, University of Al-Qadisiyah, Al Diwaniyah, Iraq

³Department of Mechanical, Aerospace and Civil Engineering, The University of Manchester, Manchester, UK

⁴Civil Engineering, York University, Toronto, Ontario, Canada

Correspondence

Rwayda Al Hamd, Abertay University School of Applied Sciences Dundee, Dundee UK.
Email: rwayda.alhamd@gmail.com

Abstract

This paper assesses the capability of using a new data-driven approach to predict the bond strength between steel rebar and concrete subjected to high temperatures. The analysis has been conducted using a novel evolutionary polynomial regression analysis (EPR-MOGA) that employs soft computing techniques, and new correlations have been proposed. The proposed correlations provide better predictions and enhanced accuracy than existing approaches, such as classical regression analysis. Based on this novel approach, the resulting correlations have achieved a lower mean absolute error (MAE), and root mean square error (RMSE), a mean (μ) close to the optimum value (1.0) and a higher coefficient of determination (R^2) compared to available correlations, which use classical regression analysis. Based on their enhanced performance, the proposed correlations can be used to obtain better optimised and more robust design calculations.

KEYWORDS

bond strength, elevated temperature, evolutionary computing, soft computing

1 | INTRODUCTION

International standards, such as the CEB/FIB Model Code 2010¹ and Eurocode 2,² provide means of evaluating concrete behaviour for structural fire design. Both simplified and more advanced methods based on tables or curves describing concrete compressive strength evolution and other properties at high temperatures are presented in these standards. Nonetheless, the existing guidelines do not address the loss of bond between the steel reinforcement and the concrete during or after exposure to high temperatures. The bond between steel rebar and concrete is critical to the structural strength of a reinforced concrete (RC) element. After an RC component is exposed to high temperatures, the bond between reinforcing steel and concrete is weakened. The main reason for this bond degradation is the reduction in concrete strength and possible plastic deformation of the embedded steel rebar.³ The reduced concrete–steel bond can significantly impact the structural behaviour of the RC members as this

affects the transfer of tensile stress.⁴ One other factor that plays a significant role in bond strength degradation is the corrosion of the steel, as it can impact the bond between the steel and concrete, causing deterioration of the structural performance.⁵ The effect of the bond subjected to elevated temperatures has been explored to some extent in the existing literature in an effort to determine the main variables that impact performance and hence develop analytical correlations to predict the bond strength.^{6–9} Nevertheless, the bond between steel and concrete at high temperatures remains one of the least studied phenomena in concrete research.¹⁰ The failure mechanism of a RC member, including the bond between the concrete and steel, is affected by heat application; this is in part due to the concrete's temperature gradient.^{10,11} Since there is a difference in heat conductivity between concrete and steel, this property can be influential during a fire because significant temperature gradients within the structural element can emerge. The resulting temperature change directly affects the compressive strength of the concrete due to the

This is an open access article under the terms of the [Creative Commons Attribution](https://creativecommons.org/licenses/by/4.0/) License, which permits use, distribution and reproduction in any medium, provided the original work is properly cited.

© 2022 The Authors. *Fire and Materials* published by John Wiley & Sons Ltd.

dehydration of the C–S–H gel and can induce thermal spalling. The following factors have been identified as causes of thermal spalling: the heating rate that the concrete experiences,¹² the incompatibility of thermal strains of components (cement paste, aggregates, steel) or layers with various temperatures and coefficients of thermal expansion,^{11,13–17} and the pore pressure build-up induced by steam ejected during the dehydration of the C–S–H gel and portlandite¹² as well as CO₂ expelled during the calcination of limestone aggregates (in cases where limestone aggregates predominate).¹⁸

When steel fibres are added to the concrete mix, the steel fibre content influences the temperature gradient as steel fibres, being distributed throughout the concrete section, distribute the heat much faster within the concrete.⁷ A variety of parameters must be considered when evaluating the performance of concrete in a structural member subjected to high temperatures. Key parameters include the exposure period, temperature degree, peak temperature, member dimensions, concrete humidity, concrete age, aggregate type, cement chemical composition, water-cement ratio (w/c) and the structural member's loading circumstances.³

The main variables that control bond strength, according to the literature,^{6–9} are the compressive strength after high-temperature exposure (f_c), the concrete age at testing (A), where fibres are used, the total volume of fibres within the concrete (V), the surface temperature at failure (T), the ratio of the duration of thermal saturation at the maximum target temperature to the minimum size of the pull-out specimen squared (Δ), the length-to-diameter ratio (l/d) (i.e., the bond length of the embedded ribbed bar to the diameter of the bar), and finally, the cover-to-diameter ratio of the embedded ribbed bar to bar diameter (c/d). Various researchers have proposed the following analytical correlations to predict the bond strength (T_b) at ambient and high temperatures. At this point, it should be highlighted that there is a very limited number of existing high-temperature correlations in the open literature: Yang et al.⁵ (equation 1), Varona et al.⁶ (equation 2), Varona et al.⁶ (equation 3).

$$T_b = \beta \sqrt{f_c(T)} \quad (1)$$

Where β can be taken as 3.5 for $T = 20^\circ\text{C}$ to 400°C and as 2.5 for $T = 600^\circ\text{C}$ to 800°C .

$$\text{For normal strength concrete; } T_b = 0.354 f_c - 0.15 \quad (2)$$

$$\text{For high strength concrete; } T_b = 0.393 f_c - 3.43 \quad (3)$$

However, the above-mentioned analytical correlations have been developed based on classical regression analysis. The current Eurocode approach adopts a simplified estimation depending on the design tensile strength of concrete using factors to simulate “good” or “poor” bond conditions. In contrast, the current developments in artificial intelligence (AI) and machine learning (ML) are increasingly becoming valuable tools for structural engineers and have the potential to develop improved design guidance.¹⁹ Implementing novel AI and progressive regression analysis approaches that use the multi-objective

evolutionary polynomial regression analysis (EPR-MOGA) may offer significant benefits to current practice. Such techniques have been successfully used in civil engineering disciplines such as geotechnical and hydraulic engineering, providing prediction correlations with improved accuracy over existing approaches.^{20–28} This new technique can produce very good predictions with less complexity than other soft computing techniques, such as genetic programming (GP) and Multivariate Adaptive Regression Splines (MARS).²⁹ It should be noted that GP generates correlations in tree structures of variable size and then performs a global search of the correlation expression; this tends to create long and complex correlations.^{30,31} On the other hand, EPR-MOGA uses a pre-specified general form of a correlation with a known number of terms (set by the user) to search for the best symbolic correlation via an evolutionary process.

Nevertheless, an extensive review of past studies showed that this approach (EPR-MOGA) has not been used to predict the bond strength at either ambient or elevated temperatures except for the specific case of underwater concrete Assaad et al.³² The analysis conducted by Assaad et al.³² focused on capturing the washout effect on the bond characteristics using regression correlations. The present work aims to implement the new approach that would provide a simple, more accurate and consistent correlation to evaluate bond strength employing EPR-MOGA, thus potentially resulting in a safer and more economical design. Towards this, the EPR-MOGA approach will be used to propose new correlations to predict the bond strength at ambient and elevated temperatures. Additionally, since the available analytical correlations have not been examined rigorously in past studies, the performance of EPR-MOGA will be compared with other commonly used analytical correlations.

2 | DEVELOPMENT OF THE METHODOLOGY

This research explores the accuracy of the EPR-MOGA in predicting rebar-to-concrete bond strength at ambient and elevated temperatures. The variables used to train and test the correlation are based on an experimental database obtained from the existing literature,⁹ and the results of EOR-MOGA will be compared to the prevalent existing analytical correlations.

2.1 | Data collection

The data used in the study is based on the database developed by Varona et al.⁹ the database included concrete with and without fibre additions. The database comprises 316 data points of the bond strength at different temperatures. Varona et al.⁶ built this database and utilised it to develop analytical regression correlations. Based on the literature review conducted, the relevant parameters that impact the bond strength (T_b) at both ambient and elevated temperatures were selected.⁶ Table 1 presents the statistics of the data obtained from Varona et al.⁹ used in this study. In addition, Figure 1 illustrates

TABLE 1 Statistics of the data used in the analyses

Statistical measure	Fibre volume fraction (V) (%)	Length to diameter (l/d)	Cover to diameter (c/d)	Age at testing (A) (days)	Δ (h/dm ²)	Temperature at the surface (T) (C°)	$f_{c(cube)}$ at 20° C (MPa)	T_b , at failure C° (MPa)
Minimum	0.00	2.00	1.78	28.00	0.33	20.00	0.38	1.06
Maximum	2.00	20.83	5.75	90.00	3.00	825.00	103.60	36.30
Mean	0.15	9.74	4.64	43.78	1.82	347.74	31.74	8.41
Standard deviation	0.45	6.04	1.26	23.41	1.04	250.02	17.76	6.27

the histograms of the frequency of input and output variables. The visual representation of the data shows a good variation between the input and output. The need for further testing in the future is also recommended.

2.2 | Multi-objective evolutionary polynomial regression analysis (EPR-MOGA)

EPR-MOGA can be defined as an intelligent computational method that uses the input data to create an innovative novel solution for practical problems.^{22,33,34} This approach is based on regression analysis and uses a genetic algorithm (GA) to produce a mathematical correlation that can describe the relationship between the physical input variables.^{30,31} The EPR-MOGA uses regression analysis and implements a GA to search for the best correlation. This GA is also enhanced by adding more than one objective to control the correlation complexity and ensure the accuracy and fitness of the new correlations.³⁵ Thus, the advantages of this regression technique over the classical regression approach are as follows:

1. The best mathematical correlation is found automatically by a search algorithm. Thus, the user needs to specify the correlation structure, the number of terms of the correlation, and the exponents' range and step, unlike classical regression analysis, where the user needs to try every possible correlation manually.
2. The EPR-MOGA overcomes the overfitting problem correlated with other regression analyses that do not include AI approaches. Overfitting usually occurs when the developed correlation learns the details of the data, including the noise; this adversely affects the performance of the developed new correlation when used to predict the results of newly generated data. This implies that the developed correlation picks the noise and the random variations in the data used in the correlation development.

To conduct the analysis, the user only needs to identify the structure of the required correlation, the range of the exponents and the number of terms. A full background description of the EPR-MOGA can be found in.^{30,31}

The performance of both the new and existing analytical correlations has been examined using statistical indicators. These indicators include the mean absolute error (MAE), root mean square error (RMSE), mean (μ), and coefficient of determination (R^2) as shown in

Equations 4–7. The same approach of accuracy examination has been used in many previous studies, albeit in a different application.^{36–41} The statistical meaning for the MAE and the RMSE values describe the best fit as the lower means. Meanwhile, the μ value is correlated with an optimum value of 1.0, any higher value can be considered as an overall overprediction of the correlation and vice versa.

$$MAE = \frac{1}{n} \sum_{i=1}^n |V_{(p)} - V_{(m)}| \quad (4)$$

$$RMSE = \sqrt{\frac{1}{n} \sum_{i=1}^n (V_{(p)} - V_{(m)})^2} \quad (5)$$

$$\mu = \frac{1}{n} \sum_{i=1}^n \left(\frac{V_{(p)}}{V_{(m)}} \right) \quad (6)$$

$$R^2 = \left(\frac{\sum_{i=1}^n (V_{(p)} - V_{(p)average}) (V_{(m)} - V_{(m)average})}{\sqrt{\sum_{i=1}^n (V_{(p)} - V_{(p)average})^2 \sum_{i=1}^n (V_{(m)} - V_{(m)average})^2}} \right)^2 \quad (7)$$

In Equations 4–7, n is the number of data points used in the assessment, $V_{(p)}$ is the predicted bond strength, and $V_{(m)}$ is the measured bond strength.

3 | DEVELOPMENT OF CORRELATIONS

The correlations proposed in the present work are developed using a multi-objective GA evolutionary polynomial regression analysis (EPR-MOGA). As previously described, a database collected from existing studies has been used in the EPR-MOGA analysis. The database has been divided into two sets: training data and testing data. The training data comprises 80% of the total data (316 data points), while the testing data takes the remaining (81 data points, i.e., [20%]) in line with.²³ The first set is used to train the correlation to develop the mathematical correlation, and the second set is used to validate the correlation. This means that only the training data has been used in the correlation development, and the testing data has been used only to assess the ability of the new correlation to predict the bond strength using a database that has not guided the correlation training. Division of the database into training and testing is carried out by shuffling the data using a random-sort function, and so forth, as available in Microsoft Excel, and then splitting the data based on the required percentages.

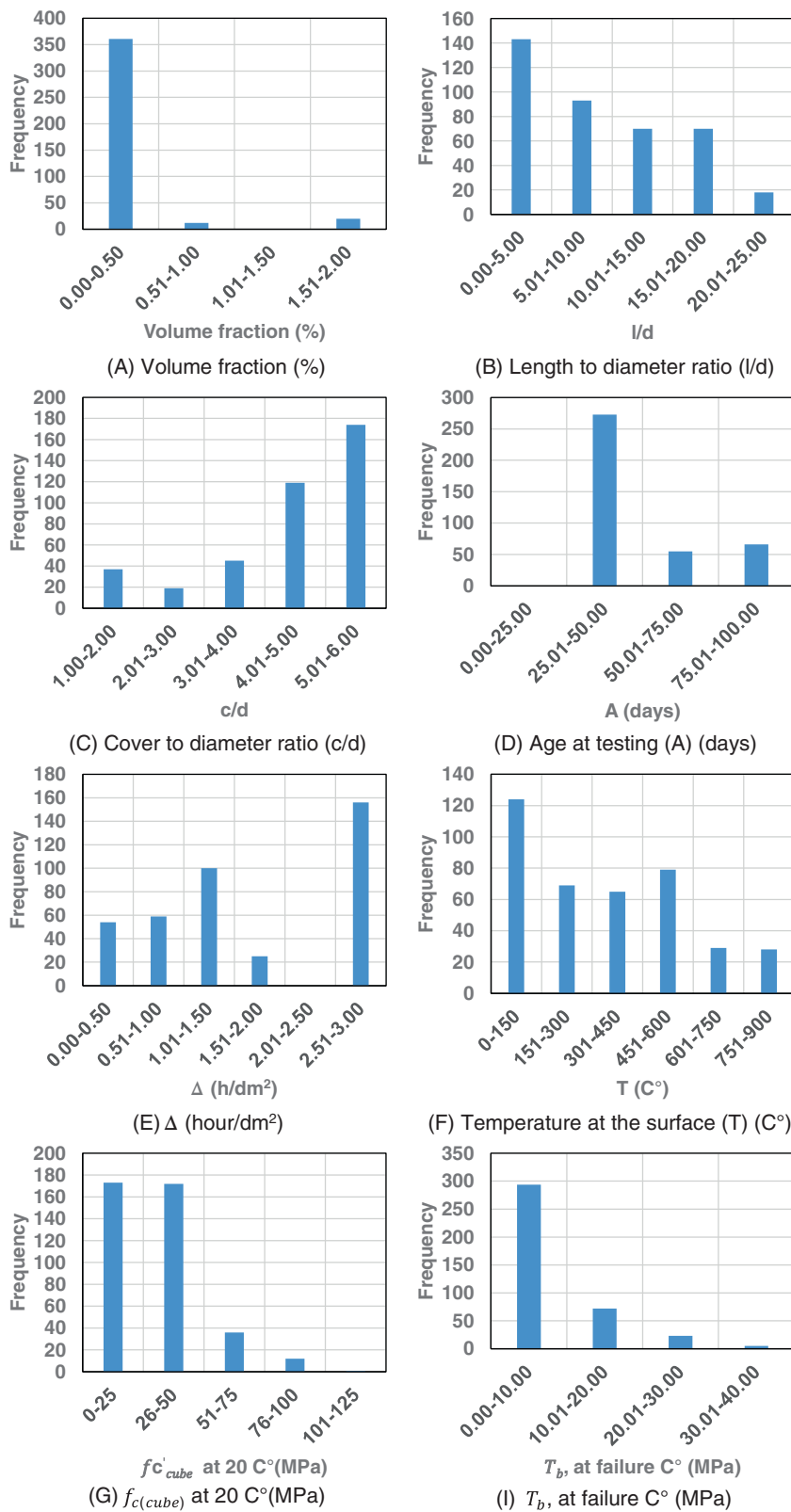


FIGURE 1 Histograms of the frequency of input and output variables

However, significant efforts have been made to ensure that the testing data is within the statistical range of the training data to avoid correlation extrapolation in the testing stage.^{23,42} Tables 2 and 3 present the training and testing statistics of the data.

The selection of the input variables assumed for the modelling is based on the relevant literature; then, a trial-and-error process is applied using the EPR-MOGA technique to fit a mathematical correlation between the input and output data to formulate the correlations.

TABLE 2 Statistics of the training data

Statistical measure	Volume fraction (%)	Length to diameter (l/d)	Cover to diameter (c/d)	Age at testing (days)	Δ (h/dm ²)	Temperature (°C)	fc,cube,T (MPa) at 20°C	Tb, at failure °C (MPa)
Minimum	0.00	2.00	1.78	28.00	0.33	20.00	0.38	1.06
Maximum	2.00	20.83	5.75	90.00	3.00	825.00	103.60	36.30
Mean	0.16	9.66	4.58	43.64	1.82	342.15	32.29	8.49
Standard deviation	0.48	6.03	1.28	23.39	1.03	250.17	18.37	6.36

TABLE 3 Statistics of the testing data

Statistical measure	Volume fraction (%)	Length to diameter (l/d)	Cover to diameter (c/d)	Age at testing (days)	Δ (h/dm ²)	Temperature (T) (°C)	fc,cube (MPa) at 20°C	Tb, at failure °C (MPa)
Minimum	0.00	2.00	1.78	28.00	0.33	20.00	5.10	1.07
Maximum	2.00	20.83	5.75	90.00	3.00	825.00	81.70	29.40
Mean	0.08	10.06	4.86	44.37	1.82	370.38	29.52	8.06
Standard deviation	0.26	6.12	1.13	23.63	1.08	249.74	14.97	5.89

TABLE 4 Statistical performance of proposed EPR Correlation 1, which considers all of the variables

Statistical measure	Training data	Testing data
MAE (MPa)	1.48	1.63
RMSE (MPa)	2.42	2.62
Mean (μ)	1.10	1.17
R ²	0.86	0.80

TABLE 5 Statistical performance of EPR Correlation 2, which considers all of the variables excluding Δ

Statistical measure	Training data	Testing data
MAE (MPa)	1.54	1.70
RMSE (MPa)	2.39	2.51
Mean (μ)	1.06	1.13
R ²	0.86	0.82

It should be noted that the trial-and-error process involved testing different correlation structures, different exponent ranges and different numbers of terms of the developed correlations. However, the search for the best fit correlation is undertaken automatically by utilising the GA.

Significant computational efforts have been provided to train correlations to predict bond strength (T_b). Three different approaches for the input data were applied with a ratio with low error and good accuracy as per Tables 4–6 with R² between 0.78–0.86, and the statistical Mean between 1.06–1.17.

It is worth stating that the authors decided to keep these small coefficients for the developed correlations (which will be discussed in

TABLE 6 Statistical performance of EPR Correlation 3, which considers all of the variables excluding Δ and the age of concrete (A)

Statistical measure	Training data	Testing data
MAE (MPa)	1.89	1.73
RMSE (MPa)	2.80	2.77
Mean (μ)	1.09	1.14
R ²	0.81	0.78

the following subsections) as the work aimed to improve the accuracy of the existing correlations.

The effect of all the main variables presented in the literature^{5–7} has been included in the developed correlation. In the case of the existing correlations, the crucial variables were often only implicitly included. In contrast, this paper explicitly proposes three correlations to include all the relevant variables and obtain more accurate correlations to predict bond strength. The suitability of the correlation to be used in practice was also considered in its development.

3.1 | Proposed EPR correlation 1

For the first proposed correlation (EPR Correlation 1), all the input variables were included in the development of the predictive correlation of the bond strength (T_b). These are the compressive strength after high-temperature exposure (f_c); the concrete age at testing (A); total volume of fibres (if present) in relation to concrete volume (V); the surface temperature at failure (T); the ratio of the duration of thermal saturation at the maximum target temperature to the minimum size of the pull-out specimen squared (Δ); the length-to-diameter ratio

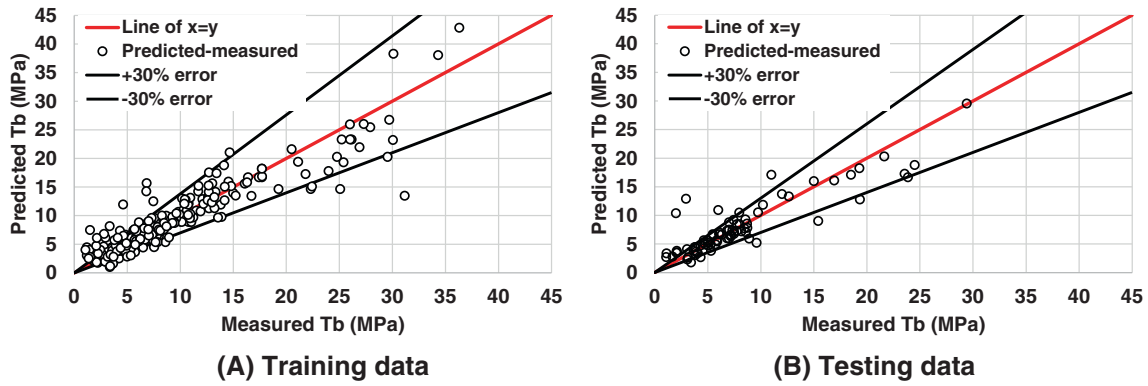


FIGURE 2 Relationship between measured and predicted T_b using the developed correlation which considers all of the variables (EPR Correlation 1)

of bond length of the embedded ribbed bar-to-bar diameter (l/d) and the ratio of the concrete cover (c) to the diameter of the embedded ribbed bar (c/d). One limitation of the dataset used is that the exact nature of the concrete and the chemical make-up of the mix (including cement type and aggregate type) are not available, these may have an influence on the bond's thermal behaviour. The best correlation obtained from the intelligence computing analysis is shown in Equation 7.

$$\begin{aligned}
 T_{b,at\ failure} = & 0.0359 \times \sqrt{\frac{c}{d}} \times \sqrt{A} \times fc, cube - 0.00000075 \times \left(\frac{c}{d}\right) \\
 & \times fc, cube \times T^2 - 0.0168 \times \sqrt{\frac{l}{d}} \times \sqrt{A} \times fc, cube \\
 & - 0.0000035 \times \sqrt{V} \times \sqrt{\Delta} \times \left(\frac{c}{d}\right) \times T^2 + 0.848 \\
 & \times \sqrt{\frac{l}{d}} \times \sqrt{V} \times \left(\frac{c}{d}\right) + 4.047
 \end{aligned} \quad (7)$$

The results from Equation 7 have been used in the predictions of T_b for the proposed EPR Correlation 1. The corresponding measured values with the no-error line and the $\pm 30\%$ error range for training and validation datasets are presented in Figure 2. The results show that the predictions are close to the no-error line for both sets and within the error range of $\pm 30\%$ for the training and testing data, demonstrating very high prediction accuracy.

The statistical performance (MAE, RMSE, μ , and R^2) for Equation 7 for both training and testing sets is shown in Table 4. The MAE for testing and validation sets (1.48 and 1.63, respectively) is very close. Similarly, the RMSE obtained demonstrates that there is no large error of predictions in the correlation, where the RMSE is equal to 2.42 and 2.62, respectively, for training and testing sets. In addition, the obtained μ value is equal to 1.10 and 1.17 for testing and training; both numbers are very close to the optimum value of 1.0. Furthermore, the R^2 ranges between 0.86 and 0.80 for both sets. In summary, many of the predictions of the EPR Correlation 1 are within the acceptable range of error. The results also indicated that the experimental data with high bond strength reported more variabilities to the

shown trend in some cases; unlike the rest of the data, as seen in Figure 2. This can be considered a limitation for the correlation, or it might be due to some experimental error, yet there is insufficient experimental data to address the current issue, indicating the need for further experimental tests.

3.2 | EPR Proposed Correlation 2

For the second proposed correlation (EPR Correlation 2), all the input variables were included in the prediction of the bond strength (T_b) except for Δ (the ratio of the duration of thermal saturation, where the water in the pores reaches boiling point, at maximum target temperature to a minimum size of pull-out specimen squared). This approach was taken to produce a practical and convenient predictive correlation as the variable Δ cannot be obtained easily for practical applications. After conducting the EPR-MOGA analysis, the best correlation obtained from the intelligence computing analysis is shown in Equation 8.

$$\begin{aligned}
 T_{b,at\ failure} = & -0.000000112 \times \frac{c}{d} \times fc, cube \times T^2 + 0.023 \times \frac{c}{d} \times fc, cube \\
 & \times \sqrt{A} - 0.000018 \times \left(\frac{c}{d}\right)^2 \times fc, cube^2 \times \sqrt{A} - 0.0087 \\
 & \times \sqrt{\frac{l}{d}} \times \sqrt{\frac{c}{d}} \times \sqrt{A} \times fc, cube + 0.0105 \times V \times fc, cube \\
 & \times \left(\frac{c}{d}\right)^2 + 2.789
 \end{aligned} \quad (8)$$

The predictions produced by this correlation are compared with the corresponding measured values in Figure 3. Based on the figure, it is evident that Equation 8 achieved high accuracy compared to the no-error line and within the $\pm 30\%$ error range for training and validation sets.

For the EPR Correlation 2, the statistical performance parameters (MAE, RMSE, μ , and R^2) are reported in Table 5. The MAE for training and testing sets (1.54 and 1.70, respectively) is very close. Conversely, the obtained RMSE expresses a low range of error in the predictions,

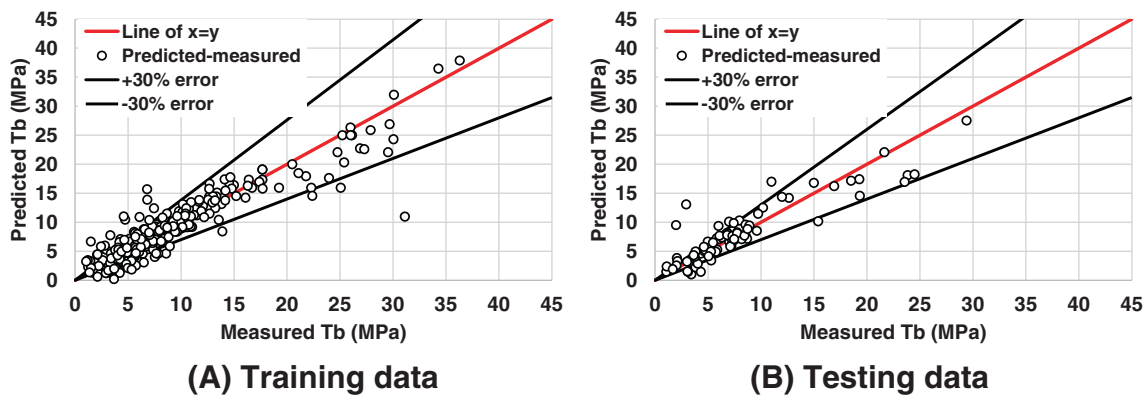


FIGURE 3 Relationship between measured and predicted T_b using the developed correlation, which considers all of the variables excluding Δ (EPR Correlation 2)

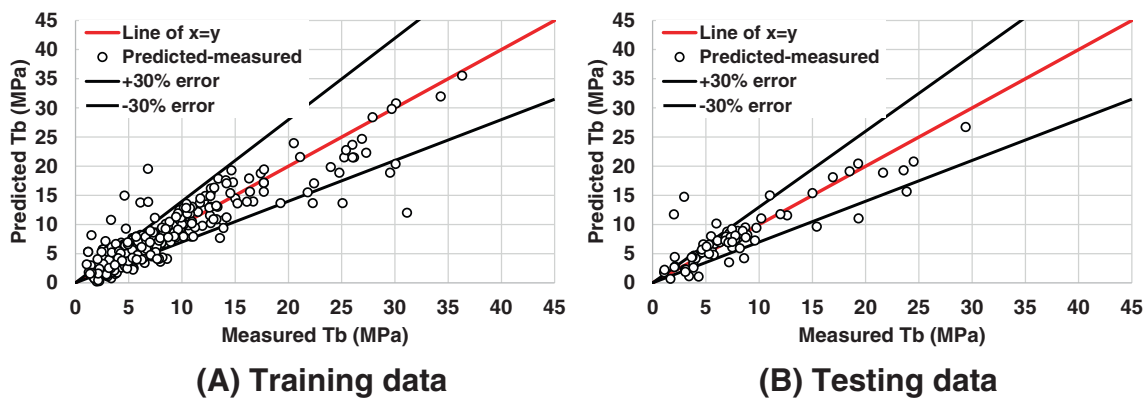


FIGURE 4 Relationship between measured and predicted T_b using the developed correlation which considers all of the variables excluding Δ and the age of concrete (EPR Correlation 3)

since the $RMSE$ is equal to 2.39 and 2.51, respectively, for training and testing sets. Last, the μ values attained (1.06, 1.13) are very close to the optimum value of 1.0 and R^2 is equal to 0.86 and 0.82 for both sets. In summary, similar to EPR Correlation 1, EPR Correlation 2 shows high accuracy for both testing and validation sets within the error range of $\pm 30\%$. The impact of higher strength variabilities of the experimental data is less apparent, as can be seen in Figure 2, indicating that eliminating the variable Δ had affected the noted trend in Correlation 1.

3.3 | EPR proposed Correlation 3

For the third proposed correlation (EPR Correlation 3), in the same way as the previous approach, the input variables were included in the prediction of the bond strength (T_b) except for Δ and the age of the concrete (A). It is difficult to have an exact time scale for the bond slippage prediction, and similarly, EPR Correlation 3 provided a more practical approach for designers. The intelligence computing analysis proposed the best correlation, as shown in Equation 9.

$$\begin{aligned}
 T_b, \text{at failure} = & 0.6926 \times f_{c, \text{cube}} - 0.00000121 \times \sqrt{\frac{c}{d}} \times \sqrt{f_{c, \text{cube}}} \times T^2 \\
 & - 0.308 \times \sqrt{\frac{l}{d}} \times f_{c, \text{cube}} + 0.015 \times \frac{l}{d} \times \sqrt{\frac{c}{d}} \times f_{c, \text{cube}} \\
 & + 0.0147 \times \sqrt{V} \times \sqrt{f_{c, \text{cube}}} \times \frac{l}{d} \times \left(\frac{c}{d}\right)^2 + 6.224
 \end{aligned} \quad (9)$$

For EPR Correlation 3, shown in Equation 9, the corresponding measured values indicate a high accuracy compared to the no-error line and within the $\pm 30\%$ error range for training and testing sets. However, this correlation seems to have less accuracy than EPR Correlation 1 and EPR Correlation 2 (see Figure 4). This shows that the concrete (A) age impacts the accuracy of the prediction of the data. When the statistical performance parameters (MAE , $RMSE$, μ , and R^2) shown in Table 6 were compared to the first two correlations (Tables 4 and 5), the first two correlations showed better results. The MAE for the training and testing sets, 1.89 and 1.73, respectively, is very close. On the other hand, the obtained $RMSE$ expresses a low range of errors in the predictions, since the $RMSE$ is equal to 2.80 and 2.77, respectively, for training and testing sets. Last, the μ , value

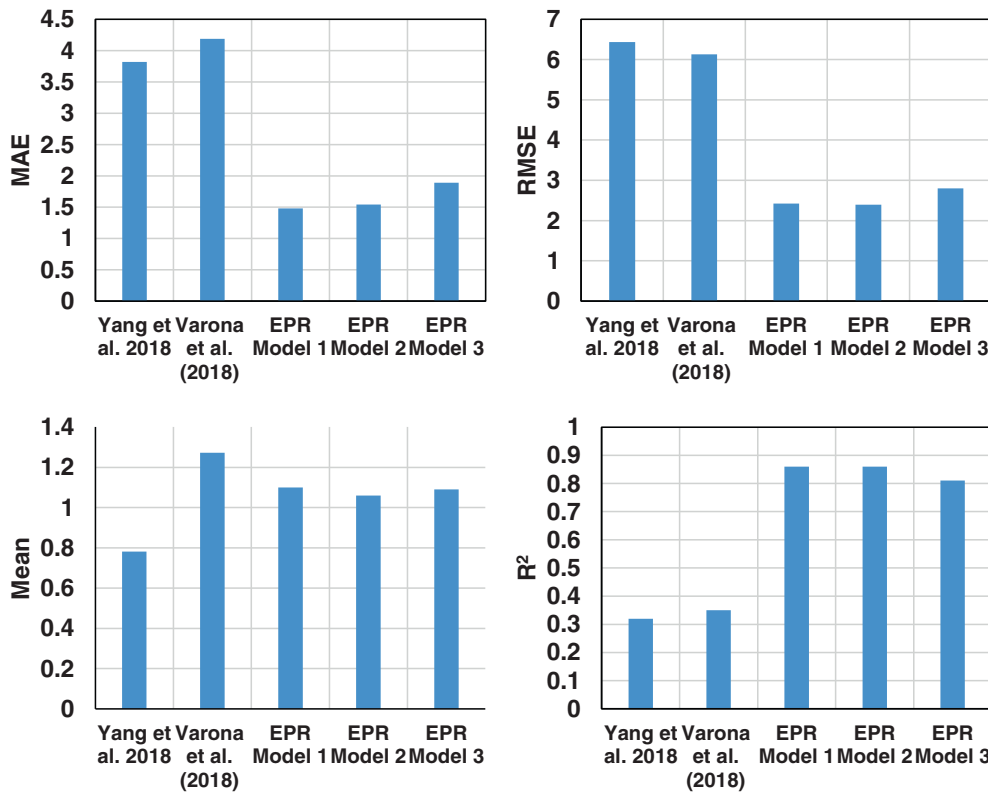


FIGURE 5 Comparison of the statistical performance of the new correlations compared with empirical correlations proposed in the literature for the training data

attained (1.09, 1.14) is very close to the optimum value of 1.0 and R^2 is between 0.81 and 0.78 for both sets. In summary, similar to EPR Correlation 1 and EPR Correlation 2, EPR Correlation 3 shows a good accuracy for both training and testing sets within the error range of $\pm 30\%$ but with a lower R^2 . Also, as with EPR Correlation 2, the elimination of Δ and A has impacted the predications of the correlation resulting in high data disturbance.

4 | COMPARISONS OF THE PERFORMANCE OF THE NEW CORRELATIONS WITH EXISTING EMPIRICAL CORRELATIONS

The statistical performance of the three correlations developed in this study was compared to the existing correlations.^{5-7,9} It should be mentioned that there is no correlation developed in the available literature that has included all the crucial variables except for the correlation developed by Varona et al.⁶ shown in Equation 10. However, that correlation has not included the effect of the ratio of the duration of the thermal parameter (Δ), which was included in EPR Correlation 1. Another shortcoming with the Varona et al. correlation is that it produces negative values in specific conditions [6], that is, for temperatures above 550°C , a 28-day plain concrete with $c/d = 5$ and l/d greater than 10, the correlation would predict a negative value of coefficient “ k_b ” due to a limitation in the CEB/FIB Model Code 2010.¹

$$T_b = k_b (f_c)^{0.639} \quad (10)$$

Where the k_b is the coefficient for plain concrete

$$k_b = k_{b,plain\ concrete} = 0.268 - 0.00101T - \frac{0.211l}{d} + \frac{0.30c}{d} + 0.0194A$$

And for the concrete with fibres

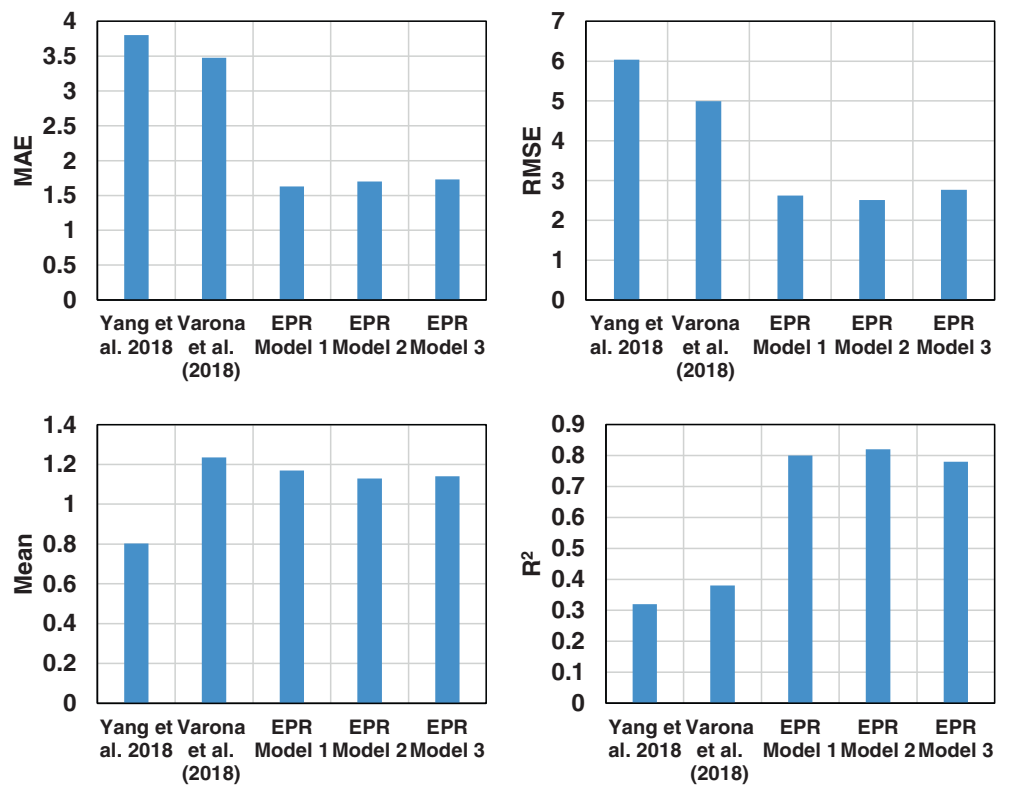
$$k_b = k_{b,plain\ concrete} - 0.187FT + 0.904VF$$

The statistical performance parameters (MAE, RMSE, μ , and R^2) are shown in Figures 5 and 6 for Equations 7-9 compared to equations 1-3 developed by Yang et al. 2018⁵ and Varona et al. 2018⁶ for both the training and the testing sets. The results show that the proposed new correlations are more accurate, achieving lower error for both sets.

The main significant difference between the developed and existing correlations is that the new correlations achieved much less MAE and RMSE for both sets. As for the mean value μ , it can be noticed that all the new correlations are much closer to the optimum value of 1.0. Finally, the new correlation returned a R^2 between 0.78-0.86; this range is very high compared to the existing correlations in the literature.^{5,7}

Ultimately, the correlation EPR Correlation 1 (Equation 8) has given the best fit for both data sets achieving high accuracy in predications, as can be seen from Figures 5 and 6. The statistical performance

FIGURE 6 Comparison of the statistical performance of the new correlations compared with existing empirical correlations for the testing data



MAE is 1.48 for training and 1.63 for testing, the *RSME* is 2.42 for training and 2.62 for testing, the μ is 1.1 for training and 1.17 for testing, and the R^2 is 0.86 for training, 0.80 for testing. This means that all the variables are needed to predict the bond strength. However, for practical reasons, EPR Correlation 2 excludes only one of the variables, that is, the ratio of the duration of thermal saturation at maximum target temperature to a minimum size of pull-out specimen squared (Δ), this correlation could be used in practice to give reliable predictions for the bond strength at elevated temperatures as the statistical performance of the correlation R^2 is 0.86 for training and 0.80 for testing, and the μ is 1.06 for training and 1.13 for testing. Nevertheless, with the third correlation from EPR Correlation 3, even if it was shown to be a less accurate prediction, the first two were still better than the other correlations proposed in the literature,⁵⁻⁷ with R^2 being 0.81 for training and 0.78 for testing; meanwhile, the R^2 for the existing correlations is below 0.50.

5 | CONCLUSIONS AND FUTURE WORK

This study applied the novel EPR-MOGA technique to predict the bond strength between concrete and steel rebar at elevated temperatures using data obtained from the literature. The results showed that much higher accuracy was achieved using the new approach. Three new correlations were developed. Consequently, the outcomes of this work provide a potentially powerful and straightforward approach for designers and have shown improved accuracy compared to existing correlations. Taking the limitations of the presented work into consideration, the following conclusions can be drawn:

1. The three proposed correlations showed accuracy better than the existing correlations in the available literature, with R^2 between 0.78 and 0.86 compared to R^2 below 0.50 for the available existing correlations.
2. The first proposed correlation, EPR Correlation 1, showed the best accuracy, including all the variables. The MAE for testing and validation sets (1.48 and 1.63, respectively) is close. Similarly, the *RMSE* obtained demonstrates no significant error in predictions in the correlation, whereby the *RMSE* is equal to 2.42 and 2.62, respectively, for training and testing sets. In addition, the obtained Mean (μ) value is equal to 1.10 and 1.17 for testing and training; both numbers are very close to the optimum value of 1.0. Furthermore, the R^2 ranges between 0.86 and 0.80 for both sets.
3. The second proposed correlation, EPR Correlation 2, showed a high accuracy after excluding one of the variables that would be difficult to obtain in practice. The statistical performance reported that the MAE for training and testing sets (1.54 and 1.70, respectively) is close. On the other hand, the obtained *RMSE* express a low range of error in the predictions since the *RMSE* is equal to 2.39 and 2.51, respectively, for training and testing sets. Last, the μ values attained (1.06, 1.13) are close to the optimum value of 1.0 and R^2 is equal to 0.86 and 0.82 for both sets.
4. In the third proposed correlation, EPR Correlation 3, the statistical performance is not as efficient as Correlations 1 and 2 but showed much better accuracy than the results obtained from the existing correlations, with the Mean μ , value attained (1.09, 1.14) approaching the optimum value of 1.0. R^2 is between 0.81 and 0.78 for both sets compared to the Mean μ value between 0.8 to 1.2 and R^2 below 0.50.

To conclude, this work has presented a coherent methodology to implement a well-established soft computing approach using an AI algorithm to develop three correlations that can be easily used in practice. Further refinement of the correlations can be undertaken in the future. Such refinements should include the introduction of more experimental data; currently, the availability of experimental data for concrete in high temperatures is limited, particularly in the case of fibre-RC.

FUNDING INFORMATION

None.

CONFLICT OF INTEREST

None declared.

DATA AVAILABILITY STATEMENT

Data derived from public domain resources.

ORCID

Rwayda Kh. S. Al Hamd  <https://orcid.org/0000-0002-8702-0279>

Saif Alzabeebee  <https://orcid.org/0000-0001-9685-5641>

Lee S. Cunningham  <https://orcid.org/0000-0002-7686-7490>

John Gales  <https://orcid.org/0000-0003-2843-2924>

REFERENCES

- CEB-FIB International Federation for Structural Concrete. *Fib Model Code 2010, 2013 fédration Internationale du béton / International Federation for Structural Concrete (Fib) Postal*. Wiley; 2010.
- EN1992-January 2. Eurocode 2: Design of Concrete Structures - Part 1-2: General Rules - Structural Fire Design, in: Eurocode 2, 2004. 2004.
- Diederichs U, Schneider U. Bond strength at high temperatures. *Mag Concr Res*. 1981;33:75-84.
- Khan MR. Post heat exposure behaviour of reinforced concrete beams. *Mag Concr Res*. 1986;38:59-66.
- Yang O, Zhang B, Yan G, Chen J. Bond performance between slightly corroded steel Bar and concrete after exposure to high temperature. *J Struct Eng*. 2018;144:4018209.
- Varona FB, Baeza FJ, Bru D, et al. Non-linear multivariable model for predicting the steel to concrete bond after high temperature exposure. *Constr Build Mater*. 2019;249:118713.
- Varona FB, Baeza FJ, Bru D, Ivorra S. Evolution of the bond strength between reinforcing steel and fibre reinforced concrete after high temperature exposure. *Constr Build Mater*. 2018;176:359-370.
- Varona FB, Baeza FJ, Ivorra S, Bru D. Experimental analysis of the loss of bond between rebars and concrete exposed to high temperatures | Análisis experimental de la pérdida de adherencia hormigón-acero en hormigones sometidos a altas temperaturas. *Dyna*. 2015;90:78-86.
- Varona FB, Baeza FJ, Bru D, Ivorra S. Database of experimental results for steel-to-concrete bond at high temperature, 2. 2020. [10.17632/CVB6BMCPMK.2](https://doi.org/10.17632/CVB6BMCPMK.2)
- Mousavi A, Hajiloo H, Green MF. Bond performance of GFRP reinforcing bars under uniform or gradient temperature distributions. *J Compos Constr*. 2021;25(6).
- Al-Hamd RKS, Gillie M, Mohamad SA, Cunningham LS. Influence of loading ratio on flat slab connections at elevated temperature: a numerical study. *Front Struct Civil Eng*. 2020;14:664-674.
- Placeholder TextBazant ZP, Kaplan MF. Concrete at high temperatures: material properties and mathematical models. 1996.
- Foti D. Prestressed slab beams subjected to high temperatures. *Compos Part B Eng*. 2014;58:242-250.
- Bailey CG, Ellobody E. Whole-building behaviour of bonded post-tensioned concrete floor plates exposed to fire. *Eng Struct*. 2009;31:1800-1810.
- Al Hamd RKS, Gillie M, Wang Y. Numerical modelling of slab-column concrete connections at elevated temperatures. *IABSE Sympos Rep*. 2017;109:3365-3369.
- Al Hamd RKS, Gillie M, Warren H, Torelli G, Stratford T, Wang Y. The effect of load-induced thermal strain on flat slab behaviour at elevated temperatures. *Fire Saf J*. 2018;97:12-18.
- Al-Hamd R, Gillie M, Cunningham LS, Warren H, Albostami AS. Novel shearhead reinforcement for slab-column connections subject to eccentric load and fire, archives of civil and mechanical. *Engineering*. 2019;19:503-524.
- Ahmed AE, Al-Shaikh AH, Arafat TI. Residual compressive and bond strengths of limestone aggregate concrete subjected to elevated temperatures. *Mag Concr Res*. 1992;44:117-125.
- Naser MZ. An engineer's guide to explainable artificial intelligence and interpretable machine learning: navigating causality, forced goodness, and the false perception of inference. *Automat Constr*. 2021;129:103821.
- Ahangar-Asr A, Javadi AA, Johari A, Chen Y. Lateral load bearing capacity modelling of piles in cohesive soils in undrained conditions: an intelligent evolutionary approach. *Appl Soft Comput J*. 2014;24:822-828.
- Ahangar Asr A, Faramarzi A, Javadi AA. An evolutionary modelling approach to predicting stress-strain behaviour of saturated granular soils. *Eng Comput*. 2018;35(8):2931-2952.
- Alzabeebee S. Dynamic response and design of a skirted strip foundation subjected to vertical vibration. *Geomech Eng*. 2020;20(4):345-358.
- Alzabeebee S, Chapman DN, Faramarzi A. Development of a novel model to estimate bedding factors to ensure the economic and robust design of rigid pipes under soil loads. *Tunnell Undergr Space Technol*. 2018;71:567-578.
- Alzabeebee S, Chapman DN, Faramarzi A. Economical design of buried concrete pipes subjected to UK standard traffic loading. *Proc Instit Civil Eng Struct Build*. 2019;172:141-156.
- Shams MA, Shahin MA, Ismail MA. Design of Stiffened Slab Foundations on reactive soils using 3D numerical modeling. *Int J Geomech*. 2020;20(7).
- Du Z, Shahin MA, El Naggar H. Design of ram-Compacted Bearing Base Piling Foundations by simple numerical modelling approach and artificial intelligence technique. *Int J Geosynthet Ground Eng*. 2021;7:41.
- Nassr A, Esmaeili-Falak M, Katebi H, Javadi A. A new approach to modeling the behavior of frozen soils. *Eng Geol*. 2018;246:82-90.
- Nassr A, Javadi A, Faramarzi A. Developing constitutive models from EPR-based self-learning finite element analysis. *Int J Numer Analyt Methods Geomech*. 2018;42:401-417.
- Alzabeebee S. Application of EPR-MOGA in computing the liquefaction-induced settlement of a building subjected to seismic shake. *Eng Comput*. 2020;38:437-448.
- Giustolisi O, Savic DA. Advances in data-driven analyses and modelling using EPR-MOGA. *J Hydroinform*. 2009;11:225-236.
- Giustolisi O, Savic DA. A symbolic data-driven technique based on evolutionary polynomial regression. *J Hydroinform*. 2006;8:207-222.
- Assaad JJ, Nasr D, Gerges N, Issa C. Use of soft computing techniques to predict the bond to reinforcing bars of underwater concrete. *Int J Civil Eng*. 2021;19:669-683.
- Zuhaira AA, Al-Hamd RKS, Alzabeebee S, Cunningham LS. Numerical investigation of skimming flow characteristics over non-uniform gabion-stepped spillways. *Innovat Infrastruct Solut*. 2021;6:225.

34. Alzabeebee S, Mohamad SA, Al-Hamd RKS. Surrogate models to predict maximum dry unit weight, optimum moisture content and California bearing ratio from grain size distribution curve. *Road Mater Pavement Des.* 2021;23:2733-2750.
35. Alani AM, Faramarzi A, Mahmoodian M, Tee KF. Prediction of sulphide build-up in filled sewer pipes. *Environ Technol.* 2014;35:1721-1728.
36. Alkroosh IS, Bahadori M, Nikraz H, Bahadori A. Regressive approach for predicting bearing capacity of bored piles from cone penetration test data. *J Rock Mech Geotech Eng.* 2015;7:584-592.
37. cGunduz Z, Arman H. Possible relationships between compression and recompression indices of a low-plasticity clayey soil. *Arab J Sci Eng: Sect B.* 2007;32:179-190.
38. Huang C-F, Li Q, Wu S-C, Liu Y, Li J-Y. Assessment of empirical equations of the compression index of muddy clay: sensitivity to geographic locality. *Arab J Geosci.* 2019;12:122.
39. Kordnaei A, Kalantary F, Kordtabar B, Mola-Abasi H. Prediction of recompression index using GMDH-type neural network based on geotechnical soil properties. *Soils Foundat.* 2015;55:1335-1345.
40. Tinoco J, Alberto A, da Venda P, Gomes Correia A, Lemos L. A novel approach based on soft computing techniques for unconfined compression strength prediction of soil cement mixtures. *Neu Comput Appl.* 2020;32:8985-8991.
41. Zhang W, Zhang R, Wu C, et al. State-of-the-art review of soft computing applications in underground excavations. *Geosci Front.* 2020; 11:1095-1106.
42. Alzabeebee S. Seismic response and design of buried concrete pipes subjected to soil loads. *Tunnell Undergr Space Technol.* 2019;93:103084.

How to cite this article: Al Hamd RKS, Alzabeebee S, Cunningham LS, Gales J. Bond behaviour of rebar in concrete at elevated temperatures: A soft computing approach. *Fire and Materials.* 2022;1-11. doi:[10.1002/fam.3123](https://doi.org/10.1002/fam.3123)